

# Verification-Aided Deep Ensemble Selection

Guy Amir, Guy Katz, and Michael Schapira

The Hebrew University of Jerusalem, Israel  
{guyam, guykatz, schapiram}@cs.huji.ac.il

**Abstract.** Deep neural networks (DNNs) have become the technology of choice for realizing a variety of complex tasks. However, as highlighted by many recent studies, even an imperceptible perturbation to a correctly classified input can lead to misclassification by a DNN. This renders DNNs vulnerable to strategic input manipulations by attackers, and also prone to oversensitivity to environmental noise. To mitigate this phenomenon, practitioners apply joint classification by an *ensemble* of DNNs. By aggregating the classification outputs of different individual DNNs for the same input, ensemble-based classification reduces the risk of misclassifications due to the specific realization of the stochastic training process of any single DNN. However, the effectiveness of a DNN ensemble is highly dependent on its members *not simultaneously erring* on many different inputs. In this case study, we harness recent advances in DNN verification to devise a methodology for identifying ensemble compositions that are less prone to simultaneous errors, even when the input is adversarially perturbed — resulting in more *robustly-accurate* ensemble-based classification. Our proposed framework uses a DNN verifier as a backend, and includes heuristics that help reduce the high complexity of directly verifying ensembles. More broadly, our work puts forth a novel universal objective for formal verification that can potentially improve the robustness of real-world, deep-learning-based systems across a variety of application domains.

## 1 Introduction

In recent years, deep learning [26] has emerged as the state-of-the-art solution for a myriad of tasks. Through the automated training of *deep neural networks* (DNNs), engineers can create systems capable of correctly handling previously unencountered inputs. DNNs excel at tasks ranging from image recognition and natural language processing to game playing and protein folding [2, 16, 64, 65], and are expected to play a key role in various complex systems [11, 34].

Despite their immense success, DNNs suffer from severe vulnerabilities and weaknesses. A prominent example is the sensitivity of DNNs to *adversarial inputs* [27, 38, 70], i.e., slight perturbations of correctly-classified inputs that result in misclassifications. The susceptibility of DNNs to input perturbations involves two risks that limit the applicability of deep learning to mission-critical tasks: (1) falling victim to strategic input manipulations by *attackers*, and (2) failing to *generalize* well in the presence of environmental noise. In light of the

above, enhancing the *robustness* of DNN-based classification to adversarial inputs while preserving *accuracy* has attracted considerable attention in recent years [10,22,51,72,86]. Informally, a classifier is *robustly accurate* (aka *astute* [77]) with respect to a given distribution over inputs, if it continues to correctly classify inputs drawn from this distribution, with high probability, even when these inputs are arbitrarily perturbed (up to some maximally allowed perturbation).

We build on a classic technique for improving classification quality [6, 42]: combining the outputs of an *ensemble* [21,30,71] of DNN-based classifiers on an input to derive a joint classification decision for that input. By incorporating the outputs of *independently-trained* DNNs, ensembles mitigate the risk of misclassification of a single DNN due to a specific realization of its stochastic training process and the specifics of its training data traversal. For a DNN ensemble to provide a meaningful improvement over utilizing a single DNN, its members should not frequently misclassify *the same* input. Consider, for instance, an extreme example, where an ensemble with  $k = 10$  members is used, but for some part of the input space, the 10 DNNs effectively behave identically, making mistakes on the exact same inputs. In this scenario, the ensemble as a whole is no more robust on this input subspace than each of its individual members. Our objective is to demonstrate how recent advances in DNN verification [31,35] can be harnessed to provide system designers and engineers with the means to avoid such scenarios, by constructing adequately diverse ensembles.

Significant progress has recently been made on formal verification techniques for DNNs [1,5,8,9,19,46,57,66,79]. The basic DNN verification query is to determine, given a DNN  $N$ , a precondition  $P$ , and a postcondition  $Q$ , whether there exists an input  $x$  such that  $P(x)$  and  $Q(N(x))$  both hold. Recent verification work has focused on *identifying* adversarial inputs to DNN-based classification, or formally proving that no such inputs exist [23,28,48]. We demonstrate the applicability of DNN verification to solving a new kind of queries, pertaining to DNN ensembles, which could significantly boost the robustness of these ensembles (as opposed to just measuring the robustness of individual DNNs). We note that despite great strides in recent years [37,48,66], even state-of-the-art DNN verification tools face severe scalability limitations. This renders solving verification queries pertaining to ensembles extremely challenging, since the complexity of this task grows exponentially with the number of ensemble members (see Section 3).

In this case-study paper, we propose and evaluate an efficient and scalable approach for verifying that different ensemble members do not tend to err simultaneously. Specifically, our scheme considers *small subsets* of ensemble members, and dispatches verification queries to seek perturbations of inputs for which *all* members in the subset err *simultaneously*. By identifying such inputs, we can assign a *mutual error score* to each subset. Using these mutual error scores, we compute, for each individual ensemble member, a *uniqueness score* that signifies how often it errs simultaneously with other ensemble members. This score can be used to detect the “weakest” ensemble members, i.e. those most prone to erring in parallel to others, and replace them with fresh DNNs — thus en-

hancing the diversity among the ensemble members, and improving the overall robust accuracy of the ensemble.

To evaluate our scheme, we implemented it as a proof-of-concept tool, and used this tool to conduct extensive experimentation on DNN ensembles for classifying digits and clothing items. Our results demonstrate that by identifying the weakest ensemble members (using verification) and replacing them, the robust accuracy of the ensemble as a whole may be significantly improved. These results showcase the potential of our approach.

The rest of the paper is organized as follows. Section 2 contains background on DNN ensembles and DNN verification. In Section 3 we present our verification-based methodology for ensemble selection, and then present our case study in Section 4. Related work is covered in Section 5, and we conclude in Section 6.

## 2 Background

**Deep Neural Networks.** A deep neural network (DNN) [26] is a directed graph, comprised of layers of nodes (also known as *neurons*). In feed-forward DNNs, data flows sequentially from the first (*input*) layer, through a sequence of intermediate (*hidden*) layers, and finally into an *output* layer. The network’s output is evaluated by assigning values to the input layer’s neurons and computing the value assignment for neurons in each of the following layers, in order, until reaching the output layer and returning its neuron values to the user. In classification networks, which are our subject matter here, each output neuron corresponds to an output *class*; and the output neuron with the highest value represents the class, or label, which the particular input is being classified as.

Fig. 1 depicts a toy DNN. It has an input layer with two neurons, followed by a *weighted sum* layer, which computes an affine transformation of values from its preceding layer. For example, for input  $V_1 = [1, -5]^T$ , the second layer’s computed values are  $V_2 = [-8, 1]^T$ . Next is a ReLU layer, which applies the ReLU function  $\text{ReLU}(x) = \max(0, x)$  to each individual neuron, resulting in  $V_3 = [0, 1]^T$ . Finally, the network’s output layer again computes an affine transformation, resulting in the output  $V_4 = [6, 3]^T$ . Thus, input  $[1, -5]^T$  is classified as the label corresponding to neuron  $v_4^1$ . For additional details, see [26].

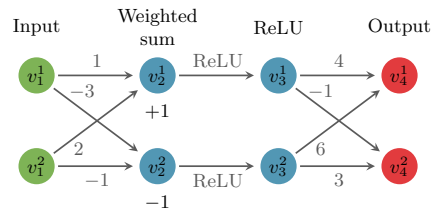


Fig. 1: A toy DNN.

**Accuracy, Robustness, and Deep Ensembles.** The weights of a DNN are determined through its training process. In supervised learning, we are provided a set of pairs  $(x_i, l_i)$  drawn according to some (unknown) distribution  $D$ , where  $x_i$  is an input point and  $l_i$  is a ground-truth label for that input. The goal is to select weights for the DNN  $N$  that maximize its *accuracy*, which is defined as:  $Pr_{(x,l) \sim D}(N(x) = l)$ . (We slightly abuse notation, and use  $N(x)$  to denote both the network’s output vector, as well as the label it assigns  $x$ .)

The training of a DNN-based classifier is typically a stochastic process. This process is affected, for example, by the initial assignment of weights to the DNN, the order in which training data is traversed, and more. A prominent method for avoiding misclassifications originating from the stochastic training of a single DNN is employing *deep ensembles*. A deep ensemble is a set  $\mathcal{E} = \{N_1, \dots, N_k\}$  of  $k$  independently-trained DNNs. The ensemble classifies an input by aggregating the individual classification outputs of its members (see Fig. 2). The collective decision is typically achieved by averaging over all members’ outputs. Ensembles have been shown to often achieve better accuracy than their individual members [6, 42, 47, 81].

A critical condition for the success of ensemble-based classifiers is that the ensemble members are not strongly correlated [43, 52, 69]. This key property is needed to avoid a scenario where many different members of the ensemble frequently make mistakes on the same input, causing the ensemble as a whole to also err on that input. Heuristics for achieving diversity across ensemble members include, e.g., training the members simultaneously with diversity-aware loss [33, 42], randomly initializing different weights for the ensemble members [40], and other methods [52, 63].

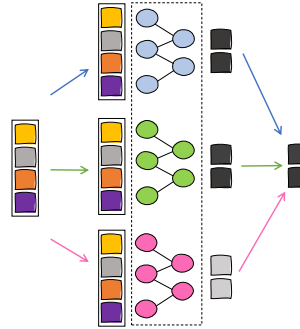


Fig. 2: An ensemble comprising three DNNs. Each input vector is independently classified by all three networks, and the results are aggregated into a final classification.

Since the discovery of adversarial inputs, practitioners have become interested in DNNs that are not only accurate but also *robustly accurate*. We say that a network  $N$  is  $\epsilon$ -robust around the point  $x$  if every input point that is at most  $\epsilon$  away from  $x$  receives the same classification as  $x$ :  $\|x' - x\| \leq \epsilon \Rightarrow N(x) = N(x')$ , where  $N(x)$  is the label assigned to  $x$ ; and the definition of accuracy is generalized to  $\epsilon$ -robust-accuracy as follows:  $Pr_{(x,l) \sim D}(\|x' - x\| \leq \epsilon \Rightarrow N(x') = l)$ . While improvements in accuracy afforded by ensembles are straightforward to measure, this is typically not so for robust accuracy, as we discuss in Section 3.

**DNN Verification.** Given a DNN  $N$ , a verification query on  $N$  specifies a precondition  $P$  on  $N$ ’s input vector  $x$ , and a postcondition  $Q$  on  $N$ ’s output vector  $N(x)$ . A DNN verifier needs to determine whether there exists a concrete input  $x_0$  that satisfies  $P(x_0) \wedge Q(N(x_0))$  (the SAT case), or not (the UNSAT case). Typically,  $P$  and  $Q$  are expressed in the logic of linear real arithmetic. For instance, the  $\epsilon$ -robustness of a DNN around a point  $x$  can be phrased as a DNN verification query, and then dispatched using existing technology [23, 35, 76]. The DNN verification problem is known to be NP-complete [36], and its complexity increases exponentially with the size of the DNN  $N$ .

### 3 Improving Robust Accuracy using Verification

#### 3.1 Directly Quantifying Robust Accuracy is Hard

In order to construct a robustly-accurate ensemble  $\mathcal{E}$  with  $k$  members, we train a set of  $n > k$  DNNs and then seek to select a subset of  $k$  DNNs that provides high robust accuracy. A straightforward approach would be to quantify the robust accuracy for all possible  $k$ -sized DNN-subsets, and then pick the best one. This, however, requires an accurate estimate of the robust accuracy of an ensemble.

A natural approach for estimating the  $\epsilon$ -robust-accuracy of a DNN is to verify, for many points in the test data, that the ensemble yields an accurate label not only on each data point itself, but also on each and every input derived from that data point via an  $\epsilon$ -perturbation [23]. The fraction of tested points for which this is indeed the case can be used to estimate the accuracy of the classifier on the underlying distribution from which the data is generated.

A similar process can be performed for an ensemble  $\mathcal{E} = \{N_1, \dots, N_k\}$ , by first constructing a single, large DNN  $N_{\mathcal{E}}$  that represents  $\mathcal{E}$ 's joint classification, and then verifying its robustness on a set of points from the test data (see Section A of the Appendix). However, this approach faces a significant scalability barrier.  $N_{\mathcal{E}}$  is (roughly)  $k$  times larger than any of the  $N_i$ 's, and since DNN verification becomes exponentially harder as the DNN size increases,  $N_{\mathcal{E}}$ 's size might render efficient verification infeasible. As we demonstrate later, this is the case even when the constituent networks themselves are fairly small. Our proposed methodology circumvents this difficulty by only solving verification queries pertaining to *very small* sets of DNNs.

#### 3.2 Mutual Error Scores and Uniqueness Scores

In general, the less likely members of an ensemble are to err simultaneously with other members, the more accurate the ensemble is. This motivates our definition of mutual error scores below.

**Definition 1 (Agreement Points).** *Given an ensemble  $\mathcal{E} = \{N_1, N_2, \dots, N_k\}$ , we say that an input point  $x_0$  is an agreement point for  $\mathcal{E}$  if there is some label  $y_0$  such that  $N_i(x_0) = y_0$  for all  $i \in [k]$ . We let  $\mathcal{E}(x_0)$  denote the label  $y_0$ .*

As we later discuss, the  $\epsilon$ -neighborhoods of agreement points are natural locations for detecting hidden tendencies of ensemble members to err together.

**Definition 2 (Mutual Errors).** *Let  $\mathcal{E}$  be an ensemble, and let  $x_0$  be an agreement point for  $\mathcal{E}$ . Let  $B_{x_0, \epsilon}$  be the  $\epsilon$ -ball around  $x_0$ ,  $B_{x_0, \epsilon} = \{x \mid \|x - x_0\|_{\infty} \leq \epsilon\}$ . We say that  $N_1$  and  $N_2$  have a mutual error in  $B$  if there exists a point  $x \in B_{x_0, \epsilon}$  such that  $N_1(x) \neq \mathcal{E}(x_0)$  and  $N_2(x) \neq \mathcal{E}(x_0)$ .*

Intuitively, if  $N_1$  and  $N_2$  have many mutual errors, incorporating both into an ensemble is a poor choice. This naturally gives rise to the following definition:

**Definition 3 (Mutual Error Scores).** Let  $A$  be a set of  $m$  agreement points in an ensemble  $\mathcal{E}$ 's input space, and let  $B_1, B_2, \dots, B_m$  denote the  $\epsilon$ -balls surrounding the points in  $A$ . Let  $N_1, N_2$  denote two members of  $\mathcal{E}$ . The mutual error score of  $N_1$  and  $N_2$  with respect to  $\mathcal{E}$  and  $A$ , denoted by  $\text{ME}_{\mathcal{E},A}(N_1, N_2)$  is defined as:

$$\text{ME}_{\mathcal{E},A}(N_1, N_2) = \frac{|\{i \mid N_1 \text{ and } N_2 \text{ have a mutual error in } B_i\}|}{m}$$

Observe that  $\text{ME}_{\mathcal{E},A}(N_1, N_2)$  is always in the range  $[0, 1]$ . The closer it is to 1, the more mutual errors  $N_1$  and  $N_2$  have.

**Definition 4 (Uniqueness Scores).** Given an ensemble  $\mathcal{E} = \{N_1, N_2, \dots, N_n\}$  and a set  $A$  of agreement points for  $\mathcal{E}$ , we define, for each ensemble member  $N_i$ , the uniqueness score for  $N_i$  with respect to  $\mathcal{E}$  and  $A$ ,  $\text{US}_{\mathcal{E},A}(N_i)$ , as:

$$\text{US}_{\mathcal{E},A}(N_i) = 1 - \frac{\sum_{j \neq i} \text{ME}_{\mathcal{E},A}(N_i, N_j)}{n - 1}$$

The uniqueness score of  $N_i$  is the complement of its average mutual error score with the other ensemble members. When this score is close to 0,  $N_i$  tends to err simultaneously with other members of the ensemble on points in  $A$ . In contrast, the closer the US score is to 1, the rarer it is for  $N_i$  to misclassify the same inputs as other members of the ensemble. Hence, ensemble members with low uniqueness scores are, intuitively, good candidates for replacement.

We point out that our definitions above can naturally be generalized to larger subsets of the ensemble members — thus measuring robust accuracy more precisely, but rendering these measurements more complex to perform in practice.

**Computing Mutual Errors.** The only computationally complex step in determining the uniqueness scores of individual ensemble members is computing the pairwise mutual errors for the ensemble. To this end, we leverage DNN verification technology. Specifically, given two ensemble members  $N_1$  and  $N_2$ , an agreement point  $a$  for the ensemble with label  $l$ , and  $\epsilon > 0$ , an appropriate DNN verification query can be formulated as follows. First, we construct from  $N_1$  and  $N_2$  a single, larger DNN  $N$ , which captures  $N_1$  and  $N_2$  simultaneously processing a shared input vector, side-by-side. This network  $N$  is then passed to a DNN verifier, with the precondition that the input be restricted to  $B$ , an  $\epsilon$ -ball around  $a$ , and the postcondition that (1) among  $N$ 's output neurons that correspond to the outputs of  $N_1$ , the neuron representing  $l$  not be maximal, and (2) among  $N$ 's output neurons that correspond to the outputs of  $N_2$ , the neuron representing  $l$  not be maximal. Such queries are supported by most available DNN verification engines. For additional details, see Section B of the Appendix.

### 3.3 Ensemble Selection using Uniqueness Scores

In order to select an ensemble of size  $k$  out of  $n$  independently trained DNN-based classifiers, our scheme starts with an arbitrary selection of  $k$  candidate members,

and then computes the uniqueness score for each member. The uniqueness scores are computed with respect to a number of pre-selected, correctly labeled, agreement points from the validation data.<sup>1</sup> The ensemble’s consensus suggests both high confidence in the selected label, and also that the classification decision is invariant to the specific realization of each DNN’s stochastic training process. Moreover, in many relevant application domains, e.g. image recognition, the correct label of a data point is expected to remain fixed under small perturbations of that point [83]. Put together, the above suggests that misclassifications of perturbations of an agreement point are expected to be quite rare for each of the ensemble members, making joint misclassifications of *the same* perturbed inputs potentially indicative of a correlation of errors by different ensemble members. Our empirical results in Section 4 show that indeed, considering relatively few agreement points from the validation set can be used to identify ensemble members that tend to err simultaneously on *other* data points.

Using the computed uniqueness scores, we identify the “weakest” member of the candidate ensemble and replace it with a fresh DNN that obtains a higher uniqueness score. This greedy search procedure is repeated for the new candidate ensemble, and so on, thus iteratively improving overall robust accuracy. The process terminates after a predefined number of iterations, when it converges (no further improvement is achievable), or when it exceeds some timeout value.

Formally, our scheme consists of the following steps: (i) independently train a set  $\mathcal{N}$  of  $n$  DNNs, and identify a set  $A$  of  $m$  agreement points for all  $n$  DNNs by sequentially checking points from the validation data set; (ii) arbitrarily choose an initial candidate ensemble  $\mathcal{E}$  of size  $k < n$ , and compute (using a verification engine backend) all mutual error scores for the DNN members comprising  $\mathcal{E}$ , with respect to  $A$ ; (iii) compute the uniqueness score for each ensemble member, and identify a DNN member  $N_l$  with a low score; (iv) identify a fresh DNN  $N_f$ , not currently in  $\mathcal{E}$ , that has a higher uniqueness score than  $N_l$ , if one exists, and replace  $N_l$  with  $N_f$ . Specifically, identify a DNN  $N_f \in \mathcal{N} \setminus \mathcal{E}$ , such that the uniqueness score of  $N_f$  with respect to the ensemble  $\mathcal{E} \setminus \{N_l\} \cup \{N_f\}$  and the point set  $A$ , namely  $\text{US}_{\mathcal{E} \setminus \{N_l\} \cup \{N_f\}, A}(N_f)$ , is maximal. If this score is greater than  $\text{US}_{\mathcal{E}, A}(N_l)$ , replace  $N_l$  with  $N_f$ , i.e. set  $\mathcal{E} := \mathcal{E} \setminus \{N_l\} \cup \{N_f\}$ ; and (v) repeat Steps (2) through (4), until no  $N_f$  is found or until the user-provided timeout or maximal iteration count are exceeded.

## 4 Case Study: MNIST and Fashion-MNIST

Below, we present the evaluation of our methodology on two datasets: the MNIST dataset for handwritten digit recognition [41], and the Fashion-MNIST dataset for clothing classification [80]. Our results for both datasets demonstrate that our technique facilitates choosing ensembles that provide high robust accuracy via relatively few, efficient verification queries.

The considered datasets are conducive for our purposes since they allow attaining high accuracy using fairly small DNNs, which enables us to *directly*

<sup>1</sup> Specifically, this is a part of the labeled data not used for training the DNNs.

*quantify* the robust accuracy of an *entire* ensemble by dispatching *otherwise intractable* verification queries (see Section 3.1). This provides the ground truth required for assessing the benefits of our approach. The scalability of our approach is very meaningful even for the relatively modest DNN sizes considered; on the MNIST data, for instance, mutual-error verification queries for two ensemble members typically took a few seconds, whereas verification queries involving the full ensemble of five networks often timed out (35% of the queries on the MNIST data timed out after 24 hours, versus only roughly 1% of the pairwise mutual-error queries). As constituent DNN sizes and ensemble sizes increase, this gap in scalability is expected to become even more significant.

Our verification queries were dispatched using the Marabou verification engine [37] (although other engines could also be used). Additional details regarding the encoding of the verification queries appear in Sections A and B of the Appendix, and additional details about the experimental results appear in Section C therein.

**MNIST.** For this part of our evaluation, we trained 10 independent DNNs  $\{N_1, \dots, N_{10}\}$  over the MNIST dataset. Each of these networks had the same architecture: an input layer of 784 neurons, followed by a fully-connected layer with 30 neurons, a ReLU layer, another fully-connected layer with 10 neurons, and a final softmax layer with 10 output neurons, corresponding to the 10 possible digit labels. All networks achieved high accuracy rates of 96.29% – 96.57% (see Table 1).

After training, we arbitrarily constructed two distinct ensembles with five DNN members each:  $\mathcal{E}_1 = \{N_1, \dots, N_5\}$  and  $\mathcal{E}_2 = \{N_6, \dots, N_{10}\}$ , with an accuracy of 97.8% and 97.3%, respectively. Notice that the ensembles achieve a higher accuracy over the test set than their individual members.

We then applied our method in an attempt to improve the robust accuracy of  $\mathcal{E}_1$ . We began by searching the validation set, and identifying 200 agreement points (the set  $A$ ), all correctly labeled as “0” (an arbitrary label) by all 10 networks. Using the 200 agreement points and 6 different perturbation sizes<sup>2</sup>  $\epsilon \in \{0.01, 0.02, 0.03, 0.04, 0.05, 0.06\}$ , we constructed 1200  $\epsilon$ -balls around the selected agreement points; and then, for every ball  $B$  and for every pair  $N_i, N_j \in \mathcal{E}_1$ , we constructed a verification query to check whether  $N_i$  and  $N_j$  have a mutual error in  $B$ . This resulted in  $\binom{5}{2} \cdot 200 \cdot 6 = 12000$  verification queries, which we dispatched using the Marabou DNN verifier [37] (each query ran with a 2-hour timeout limit). Finally, we used the results to compute the uniqueness score for each network in  $\mathcal{E}_1$ ; these results, which appear briefly in Table 1 (for  $\epsilon = 0.02$ ) and appear in full in Table 3 of the Appendix, clearly show that two of the members,  $N_2$  and  $N_5$ , are each relatively prone to erring simultaneously with the remaining four members of  $\mathcal{E}_1$ .

Next, we began searching the remaining networks,  $N_6, \dots, N_{10}$ , for good replacements for  $N_2$  and  $N_5$ . Specifically, we looked for networks that obtained higher US scores than  $N_2$  and  $N_5$ . To achieve this, we began modifying  $\mathcal{E}_1$ , each

<sup>2</sup>  $\epsilon$  values which are too small, or too large, render the queries trivial. Thus, we found it useful to use a varied selection of  $\epsilon$  values.



Table 1: Accuracy and uniqueness scores for the MNIST networks. Uniqueness scores are measured with respect to the ensemble (either  $\mathcal{E}_1$  or  $\mathcal{E}_2$ ).

	$\mathcal{E}_1$					$\mathcal{E}_2$				
	$N_1$	$N_2$	$N_3$	$N_4$	$N_5$	$N_6$	$N_7$	$N_8$	$N_9$	$N_{10}$
Accuracy	96.42%	96.55%	96.40%	96.46%	96.29%	96.44%	96.48%	96.57%	96.51%	96.46%
US	90.75%	<b>88.38%</b>	90.63%	92.13%	<b>88.63%</b>	97.38%	96.75%	97.5%	<b>98.88%</b>	<b>97.75%</b>

time removing either  $N_2$  or  $N_5$ , replacing them with one of the remaining networks, and computing the uniqueness scores for the new members (with respect to the four remaining original networks). We observed that for both  $N_2$  and  $N_5$ , network  $N_9$  was a good replacement, obtaining very high US values. For additional details, see Section C of the Appendix.

Finally, to evaluate the effect of our changes to  $\mathcal{E}_1$ , we constructed the two new ensembles,  $\mathcal{E}_1^{2 \rightarrow 9} = \{N_1, N_9, N_3, N_4, N_5\}$  and  $\mathcal{E}_1^{5 \rightarrow 9} = \{N_1, N_2, N_3, N_4, N_9\}$ . Then, we sampled 200 random input points from the test set (these need not have the same output label, nor be agreement points for the ensemble). For each sample, we created a verification query to check the robust accuracy of the new ensembles around the point, compared to the original ensemble. The results are plotted in Fig. 3, and indicate that the new ensembles demonstrated *significantly higher* robust accuracy on the tested points. These results validate our claim that a scoring metric based on agreement points is useful in improving the ensemble’s robustness also on other, “harder” input points. Our analysis also indicates that the improved robustness results originated not only from  $\epsilon$ -balls around inputs labeled as “0”, but from other labels as well. In fact, the gain in robustness was not just in quantity, but also in quality: for almost all cases, whenever  $\mathcal{E}_1$  proved robust around an input, so did  $\mathcal{E}_1^{2 \rightarrow 9}$  and  $\mathcal{E}_1^{5 \rightarrow 9}$ . This indicates that the improved robustness originated from inputs on which  $\mathcal{E}_1$  was prone to err.

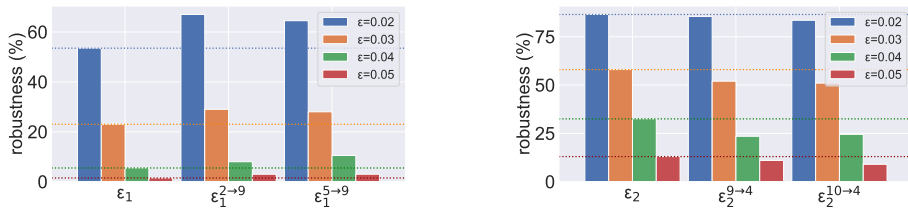


Fig. 3: The average robust accuracy scores for our original and modified ensembles. The results for  $\epsilon = 0.01$  and  $\epsilon = 0.06$  are trivial (the ensembles achieve near-perfect or near-zero robustness), and are omitted to reduce clutter.

Next, we turned our attention to  $\mathcal{E}_2$ , and computed the uniqueness scores for each of its members (see Table 1). This time we conducted a “reverse” ex-

periment: we identified the two *best* members of  $\mathcal{E}_2$ , i.e. the two networks that had the highest uniqueness scores, and were consequently the least prone to simultaneous errors. These turned out to be networks  $N_9$  and  $N_{10}$ . Next, we replaced each of these networks with each of the networks  $\{N_1, \dots, N_5\}$ , in order to identify a network that, when inserted into  $\mathcal{E}_2$ , achieved a lower score than  $N_9$  and  $N_{10}$ .  $N_4$  turned out to be such a network. We created the two modified ensembles,  $\mathcal{E}_2^{9 \rightarrow 4} = \{N_6, N_7, N_8, N_4, N_{10}\}$  and  $\mathcal{E}_2^{10 \rightarrow 4} = \{N_6, N_7, N_8, N_9, N_4\}$ , and compared their robust accuracy to that of  $\mathcal{E}_2$  on 200 random points from the test set. The results, depicted in Fig. 3, indicate that the ensemble’s robust accuracy decreased significantly, as expected.

**Fashion-MNIST.** For the second part of our evaluation, we trained 10 independent DNNs  $\{N_{11}, \dots, N_{20}\}$  over Fashion-MNIST. Each DNN had the same architecture as the MNIST-trained DNNs, and achieved an accuracy of 87.05%–87.53% (see Table 8 of the Appendix). We arbitrarily constructed two distinct ensembles,  $\mathcal{E}_3 = \{N_{11}, \dots, N_{15}\}$  and  $\mathcal{E}_4 = \{N_{16}, \dots, N_{20}\}$ , with an accuracy of 88.22% and 88.48%, respectively.

Next, we again computed the US values of each of the networks. The results, which appear in full in Table 8 of the Appendix, indicated a high variance among the uniqueness scores of the members of  $\mathcal{E}_4$ , as compared to the relatively similar scores of  $\mathcal{E}_3$ ’s members. We thus chose to focus on  $\mathcal{E}_4$ . Based on the computed US values, we identified  $N_{20}$  as its least unique DNN; and, by replacing  $N_{20}$  with each of the five networks not currently in  $\mathcal{E}_4$ , identified that  $N_{15}$  is a good candidate for replacing  $N_{20}$ . Performing our validation step over  $\mathcal{E}_4^{20 \rightarrow 15}$  revealed that its robust accuracy has indeed increased. Running the “reverse” experiment, in which  $\mathcal{E}_4$ ’s most unique member is replaced with a worse candidate, led us to consider the ensemble  $\mathcal{E}_4^{18 \rightarrow 13}$ , which indeed demonstrated lower robust accuracy than the original ensemble. For more details, see Section C of the Appendix.

For the final step of our experiment, we used our approach to iteratively switch two members of an ensemble. Specifically, after creating  $\mathcal{E}_4^{20 \rightarrow 15}$ , which had higher robust accuracy than  $\mathcal{E}_4$ , we re-computed the US scores of its members, and identified again the least unique member — in this case,  $N_{16}$ . Per our computation, the best candidate for replacing it was  $N_{12}$ . The resulting ensemble, namely  $\mathcal{E}_4^{20 \rightarrow 15, 16 \rightarrow 12}$ , indeed demonstrated higher robust accuracy than its predecessors. Performing another iteration of the “reverse” experiment yielded ensemble  $\mathcal{E}_4^{18 \rightarrow 13, 17 \rightarrow 11}$ , with poorer robust accuracy. The results appear in Fig. 4. (The only discrepancy, namely the robust accuracy of  $\mathcal{E}_4^{20 \rightarrow 15}$  being lower than that of  $\mathcal{E}_4$  for  $\epsilon = 0.04$ , is due to time-outs).

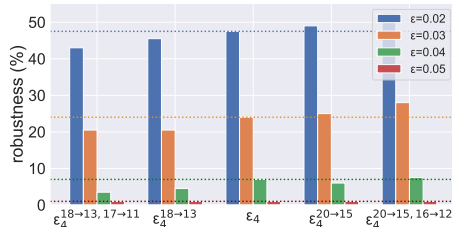


Fig. 4: The original ensemble  $\mathcal{E}_4$  (center), ensembles modified to gain robust accuracy (right), and ensembles modified to reduce robust accuracy (left).

## 5 Related Work

Due to the pervasiveness of adversarial inputs [20, 27, 50, 55, 56, 70, 87], the machine learning community has put a great deal of effort into measuring and improving the robustness of networks [14, 15, 22, 29, 44, 49, 58, 61, 62, 78, 84]. The formal methods community has also been looking into the problem, by devising scalable DNN verification, optimization and monitoring techniques [1, 4, 5, 7–9, 12, 19, 32, 45, 46, 54, 57, 60, 66, 79, 85]. Our approach uses a DNN verifier as a backend, and its scalability would improve as these verifiers become more scalable.

Obtaining DNN specifications to be verified is a difficult problem. While some studies have successfully applied verification to properties formulated by domain-specific experts [3, 18, 35, 68], most research has been focusing on *universal properties*, that pertain to every DNN-based system; specifically, local adversarial robustness [13, 28, 48, 66], fairness properties [74], network simplification [24] and modification [17, 25, 59, 67, 75, 82], and watermark resilience [25]. Through our case study, we demonstrate the applicability of DNN verification to a new class of universal properties.

## 6 Conclusion

In this case-study paper, we demonstrate a novel technique for assessing a deep ensemble’s robust accuracy through the use of DNN verification. To mitigate the difficulty inherent to verifying large ensembles, our approach considers small subsets of networks, and computes for each ensemble member a score that indicates its tendency to make the same errors as other ensemble members. These scores allow us to iteratively improve the robust accuracy of the ensemble, replacing weaker networks with stronger ones. Our empiric evaluation indicates the high practical potential of our approach; and, more broadly, we view this work as a part of the ongoing endeavor for demonstrating the real-world usefulness of DNN verification, by identifying additional, universal, DNN specifications.

**Acknowledgements.** We thank Haoze Wu for his contribution to this project. The first two authors were partially supported by the Israel Science Foundation (grant number 683/18) and the Center for Interdisciplinary Data Science Research at The Hebrew University of Jerusalem. The third author was partially supported by funding from Huawei.

## References

1. P. Alamdari, G. Avni, T. Henzinger, and A. Lukina. Formal Methods with a Touch of Magic. In *Proc. 20th Int. Conf. on Formal Methods in Computer-Aided Design (FMCAD)*, pages 138–147, 2020.
2. M. AlQuraishi. AlphaFold at CASP13. *Bioinformatics*, 35(22):4862–4865, 2019.
3. G. Amir, M. Schapira, and G. Katz. Towards Scalable Verification of Deep Reinforcement Learning. In *Proc. 21st Int. Conf. on Formal Methods in Computer-Aided Design (FMCAD)*, pages 193–203, 2021.

4. G. Amir, H. Wu, C. Barrett, and G. Katz. An SMT-Based Approach for Verifying Binarized Neural Networks. In *Proc. 27th Int. Conf. on Tools and Algorithms for the Construction and Analysis of Systems (TACAS)*, pages 203–222, 2021.
5. G. Anderson, S. Pailoor, I. Dillig, and S. Chaudhuri. Optimization and Abstraction: a Synergistic Approach for Analyzing Neural Network Robustness. In *Proc. 40th ACM SIGPLAN Conf. on Programming Languages Design and Implementations (PLDI)*, pages 731–744, 2019.
6. O. Araque, I. Corcuera-Platas, J. Sánchez-Rada, and C. Iglesias. Enhancing Deep Learning Sentiment Analysis with Ensemble Techniques in Social Applications. *Expert Systems with Applications*, 77:236–246, 2017.
7. P. Ashok, V. Hashemi, J. Kretinsky, and S. Mohr. DeepAbstract: Neural Network Abstraction for Accelerating Verification. In *Proc. 18th Int. Symp. on Automated Technology for Verification and Analysis (ATVA)*, pages 92–107, 2020.
8. G. Avni, R. Bloem, K. Chatterjee, H. T., B. Konighofer, and S. Pranger. Run-Time Optimization for Learned Controllers through Quantitative Games. In *Proc. 31st Int. Conf. on Computer Aided Verification (CAV)*, pages 630–649, 2019.
9. T. Baluta, S. Shen, S. Shinde, K. Meel, and P. Saxena. Quantitative Verification of Neural Networks and its Security Applications. In *Proc. ACM SIGSAC Conf. on Computer and Communications Security (CCS)*, pages 1249–1264, 2019.
10. R. Bhattacharjee, S. Jha, and K. Chaudhuri. Sample Complexity of Robust Linear Classification on Separated Data. In *Proc. 38th Int. Conf. on Machine Learning (ICML)*, pages 884–893, 2021.
11. M. Bojarski, D. Del Testa, D. Dworakowski, B. Firner, B. Flepp, P. Goyal, L. Jackel, M. Monfort, U. Muller, J. Zhang, X. Zhang, J. Zhao, and K. Zieba. End to End Learning for Self-Driving Cars, 2016. Technical Report. <http://arxiv.org/abs/1604.07316>.
12. R. Bunel, I. Turkaslan, P. Torr, P. Kohli, and P. Mudigonda. A Unified View of Piecewise Linear Neural Network Verification. In *Proc. 32nd Conf. on Neural Information Processing Systems (NeurIPS)*, pages 4795–4804, 2018.
13. N. Carlini, G. Katz, C. Barrett, and D. Dill. Provably Minimally-Distorted Adversarial Examples, 2017. Technical Report. <https://arxiv.org/abs/1709.10207>.
14. M. Cisse, P. Bojanowski, E. Grave, Y. Dauphin, and N. Usunier. Parseval Networks: Improving Robustness to Adversarial Examples. In *Proc. 34th Int. Conf. on Machine Learning (ICML)*, pages 854–863, 2017.
15. J. Cohen, E. Rosenfeld, and Z. Kolter. Certified Adversarial Robustness via Randomized Smoothing. In *Proc. 36th Int. Conf. on Machine Learning (ICML)*, pages 1310–1320, 2019.
16. R. Collobert, J. Weston, L. Bottou, M. Karlen, K. Kavukcuoglu, and P. Kuksa. Natural Language Processing (Almost) from Scratch. *Journal of Machine Learning Research (JMLR)*, 12:2493–2537, 2011.
17. G. Dong, J. Sun, J. Wang, X. Wang, and T. Dai. Towards Repairing Neural Networks Correctly, 2020. Technical Report. <http://arxiv.org/abs/2012.01872>.
18. S. Dutta, X. Chen, and S. Sankaranarayanan. Reachability Analysis for Neural Feedback Systems using Regressive Polynomial Rule Inference. In *Proc. 22nd ACM Int. Conf. on Hybrid Systems: Computation and Control (HSCC)*, 2019.
19. R. Ehlers. Formal Verification of Piece-Wise Linear Feed-Forward Neural Networks. In *Proc. 15th Int. Symp. on Automated Technology for Verification and Analysis (ATVA)*, pages 269–286, 2017.
20. H. Fawaz, G. Forestier, J. Weber, L. Idoumghar, and P.-A. Muller. Adversarial Attacks on Deep Neural Networks for Time Series Classification. In *Proc. Int. Joint Conf. on Neural Networks (IJCNN)*, pages 1–8, 2019.

21. S. Fort, H. Hu, and B. Lakshminarayanan. Deep Ensembles: A Loss Landscape Perspective, 2019. Technical Report. <http://arxiv.org/abs/1912.02757>.
22. Y. Ganin, E. Ustinova, H. Ajakan, P. Germain, H. Larochelle, F. Laviolette, M. Marchand, and V. Lempitsky. Domain-Adversarial Training of Neural Networks. *Journal of Machine Learning Research (JMLR)*, 17(1):2096–2030, 2016.
23. T. Gehr, M. Mirman, D. Drachler-Cohen, E. Tsankov, S. Chaudhuri, and M. Vechev. AI2: Safety and Robustness Certification of Neural Networks with Abstract Interpretation. In *Proc. 39th IEEE Symposium on Security and Privacy (S&P)*, 2018.
24. S. Gokulanathan, A. Feldsher, A. Malca, C. Barrett, and G. Katz. Simplifying Neural Networks using Formal Verification. In *Proc. 12th NASA Formal Methods Symposium (NFM)*, pages 85–93, 2020.
25. B. Goldberger, Y. Adi, J. Keshet, and G. Katz. Minimal Modifications of Deep Neural Networks using Verification. In *Proc. 23rd Int. Conf. on Logic for Programming, Artificial Intelligence and Reasoning (LPAR)*, pages 260–278, 2020.
26. I. Goodfellow, Y. Bengio, and A. Courville. *Deep Learning*. MIT Press, 2016.
27. I. Goodfellow, J. Shlens, and C. Szegedy. Explaining and Harnessing Adversarial Examples, 2014. Technical Report. <http://arxiv.org/abs/1412.6572>.
28. D. Gopinath, G. Katz, C. Păsăreanu, and C. Barrett. DeepSafe: A Data-driven Approach for Checking Adversarial Robustness in Neural Networks. In *Proc. 16th. Int. Symp. on Automated Technology for Verification and Analysis (ATVA)*, pages 3–19, 2018.
29. B. Han, Q. Yao, X. Yu, G. Niu, M. Xu, W. Hu, I. Tsang, and M. Sugiyama. CO-Teaching: Robust Training of Deep Neural Networks with Extremely Noisy Labels, 2018. Technical Report. <http://arxiv.org/abs/1804.06872>.
30. L. Hansen and P. Salamon. Neural Network Ensembles. *IEEE Transactions on Pattern Analysis and Machine Intelligence*, 12(10):993–1001, 1990.
31. X. Huang, M. Kwiatkowska, S. Wang, and M. Wu. Safety Verification of Deep Neural Networks. In *Proc. 29th Int. Conf. on Computer Aided Verification (CAV)*, pages 3–29, 2017.
32. Y. Jacoby, C. Barrett, and G. Katz. Verifying Recurrent Neural Networks using Invariant Inference. In *Proc. 18th Int. Symposium on Automated Technology for Verification and Analysis (ATVA)*, pages 57–74, 2020.
33. S. Jain, G. Liu, J. Mueller, and D. Gifford. Maximizing Overall Diversity for Improved Uncertainty Estimates in Deep Ensembles. In *Proc. 34th AAAI Conf. on Artificial Intelligence (AAAI)*, pages 4264–4271, 2020.
34. K. Julian, J. Lopez, J. Brush, M. Owen, and M. Kochenderfer. Policy Compression for Aircraft Collision Avoidance Systems. In *Proc. 35th Digital Avionics Systems Conf. (DASC)*, pages 1–10, 2016.
35. G. Katz, C. Barrett, D. Dill, K. Julian, and M. Kochenderfer. Reluplex: An Efficient SMT Solver for Verifying Deep Neural Networks. In *Proc. 29th Int. Conf. on Computer Aided Verification (CAV)*, pages 97–117, 2017.
36. G. Katz, C. Barrett, D. Dill, K. Julian, and M. Kochenderfer. Reluplex: a Calculus for Reasoning about Deep Neural Networks. *Formal Methods in System Design (FMSD)*, 2021.
37. G. Katz, D. Huang, D. Ibeling, K. Julian, C. Lazarus, R. Lim, P. Shah, S. Thakoor, H. Wu, A. Zeljić, D. Dill, M. Kochenderfer, and C. Barrett. The Marabou Framework for Verification and Analysis of Deep Neural Networks. In *Proc. 31st Int. Conf. on Computer Aided Verification (CAV)*, pages 443–452, 2019.
38. A. Kurakin, I. Goodfellow, and S. Bengio. Adversarial Examples in the Physical World, 2016. Technical Report. <http://arxiv.org/abs/1607.02533>.

39. O. Lahav and G. Katz. Pruning and Slicing Neural Networks using Formal Verification. In *Proc. 21st Int. Conf. on Formal Methods in Computer-Aided Design (FMCAD)*, pages 183–192, 2021.
40. B. Lakshminarayanan, A. Pritzel, and C. Blundell. Simple and Scalable Predictive Uncertainty Estimation using Deep Ensembles, 2016. Technical Report. <https://arxiv.org/abs/1612.01474>.
41. Y. LeCun. The MNIST Database of Handwritten Digits, 1998. <http://yann.lecun.com/exdb/mnist/>.
42. S. Lee, S. Purushwalkam, M. Cogswell, D. Crandall, and D. Batra. Why M Heads are Better than One: Training a Diverse Ensemble of Deep Networks, 2015. Technical Report. <https://arxiv.org/abs/1511.06314>.
43. S. Lee, S. Purushwalkam Shiva Prakash, M. Cogswell, V. Ranjan, D. Crandall, and D. Batra. Stochastic Multiple Choice Learning for Training Diverse Deep Ensembles. In *Proc. Advances in Neural Information Processing Systems (NeurIPS)*, 2016.
44. H. Liu, M. Long, J. Wang, and M. Jordan. Transferable Adversarial Training: A General Approach to Adapting Deep Classifiers. In *Proc. 36th Int. Conf. on Machine Learning (ICML)*, pages 4013–4022, 2019.
45. A. Lomuscio and L. Maganti. An Approach to Reachability Analysis for Feed-Forward ReLU Neural Networks, 2017. Technical Report. <http://arxiv.org/abs/1706.07351>.
46. A. Lukina, C. Schilling, and T. Henzinger. Into the Unknown: Active Monitoring of Neural Networks. In *Proc. 21st Int. Conf. on Runtime Verification (RV)*, pages 42–61, 2021.
47. Z. Lyu, N. Gutierrez, A. Rajguru, and W. Beksi. Probabilistic Object Detection via Deep Ensembles. In *Proc. European Conf. on Computer Vision (ECCV)*, pages 67–75, 2020.
48. Z. Lyu, C.-Y. Ko, Z. Kong, N. Wong, D. Lin, and L. Daniel. Fastened Crown: Tightened Neural Network Robustness Certificates. In *Proc. 34th AAAI Conf. on Artificial Intelligence (AAAI)*, pages 5037–5044, 2020.
49. A. Madry, A. Makelov, L. Schmidt, D. Tsipras, and A. Vladu. Towards Deep Learning Models Resistant to Adversarial Attacks, 2017. Technical Report. <http://arxiv.org/abs/1706.06083>.
50. S.-M. Moosavi-Dezfooli, A. Fawzi, and P. Frossard. DeepFool: A Simple and Accurate Method to Fool Deep Neural Networks. In *Proc. IEEE Conf. on Computer Vision and Pattern Recognition (CVPR)*, 2016.
51. M. Moshkovitz, Y.-Y. Yang, and K. Chaudhuri. Connecting Interpretability and Robustness in Decision Trees through Separation. In *Proc. 38th Int. Conf. on Machine Learning (ICML)*, pages 7839–7849, 2021.
52. G. Nam, J. Yoon, Y. Lee, and J. Lee. Diversity Matters When Learning From Ensembles. In *Proc. Advances in Neural Information Processing Systems (NeurIPS)*, 2021.
53. N. Narodytska, S. Kasiviswanathan, L. Ryzhyk, M. Sagiv, and T. Walsh. Verifying Properties of Binarized Deep Neural Networks, 2017. Technical Report. <http://arxiv.org/abs/1709.06662>.
54. M. Ostrovsky, C. Barrett, and G. Katz. An Abstraction-Refinement Approach to Verifying Convolutional Neural Networks, 2022. Technical Report. <https://arxiv.org/abs/2201.01978>.
55. N. Papernot, P. McDaniel, I. Goodfellow, S. Jha, Z. Celik, and A. Swami. Practical Black-Box Attacks against Machine Learning. In *Proc. ACM on Asia Conf. on Computer and Communications Security*, pages 506–519, 2017.

56. N. Papernot, P. McDaniel, S. Jha, M. Fredrikson, Z. Celik, and A. Swami. The Limitations of Deep Learning in Adversarial Settings. In *IEEE European Symposium on Security and Privacy (EuroS&P)*, pages 372–387, 2016.
57. P. Prabhakar and Z. Afzal. Abstraction Based Output Range Analysis for Neural Networks, 2020. Technical Report. <https://arxiv.org/abs/2007.09527>.
58. C. Qin, J. Martens, S. Gowal, D. Krishnan, K. Dvijotham, A. Fawzi, S. De, R. Stanforth, and P. Kohli. Adversarial Robustness through Local Linearization, 2019. Technical Report. <http://arxiv.org/abs/1907.02610>.
59. I. Refaeli and G. Katz. Minimal Multi-Layer Modifications of Deep Neural Networks, 2021. Technical Report. <https://arxiv.org/abs/2110.09929>.
60. W. Ruan, X. Huang, and M. Kwiatkowska. Reachability Analysis of Deep Neural Networks with Provable Guarantees. In *Proc. 27th Int. Joint Conf. on Artificial Intelligence (IJCAI)*, 2018.
61. A. Shafahi, M. Najibi, A. Ghiasi, Z. Xu, J. Dickerson, C. Studer, L. Davis, G. Taylor, and T. Goldstein. Adversarial Training for Free!, 2019. Technical Report. <http://arxiv.org/abs/1904.12843>.
62. A. Shafahi, P. Saadatpanah, C. Zhu, A. Ghiasi, C. Studer, D. Jacobs, and T. Goldstein. Adversarially Robust Transfer Learning, 2019. Technical Report. <http://arxiv.org/abs/1905.08232>.
63. C. Shui, A. Mozafari, J. Marek, I. Hedhli, and C. Gagné. Diversity Regularization in Deep Ensembles, 2018. Technical Report. <http://arxiv.org/abs/1802.07881>.
64. D. Silver, A. Huang, C. Maddison, A. Guez, L. Sifre, G. Van Den Driessche, J. Schrittwieser, I. Antonoglou, V. Panneershelvam, M. Lanctot, and S. Dieleman. Mastering the Game of Go with Deep Neural Networks and Tree Search. *Nature*, 529(7587):484–489, 2016.
65. K. Simonyan and A. Zisserman. Very Deep Convolutional Networks for Large-Scale Image Recognition, 2014. Technical Report. <http://arxiv.org/abs/1409.1556>.
66. G. Singh, T. Gehr, M. Puschel, and M. Vechev. An Abstract Domain for Certifying Neural Networks. In *Proc. 46th ACM SIGPLAN Symposium on Principles of Programming Languages (POPL)*, 2019.
67. M. Sotoudeh and A. Thakur. Correcting Deep Neural Networks with Small, Generalizing Patches. In *Workshop on Safety and Robustness in Decision Making*, 2019.
68. X. Sun, K. H., and Y. Shoukry. Formal Verification of Neural Network Controlled Autonomous Systems. In *Proc. 22nd ACM Int. Conf. on Hybrid Systems: Computation and Control (HSCC)*, 2019.
69. M. Svensén and C. M. Bishop. *Pattern Recognition and Machine Learning*. Springer Berlin/Heidelberg, Germany, 2007.
70. C. Szegedy, W. Zaremba, I. Sutskever, J. Bruna, D. Erhan, I. Goodfellow, and R. Fergus. Intriguing Properties of Neural Networks, 2013. Technical Report. <http://arxiv.org/abs/1312.6199>.
71. S. Tao. Deep Neural Network Ensembles. In *Int. Conf. on Machine Learning, Optimization, and Data Science*, pages 1–12, 2019.
72. F. Tramer, A. Kurakin, N. Papernot, I. Goodfellow, D. Boneh, and P. McDaniel. Ensemble Adversarial Training: Attacks and Defenses, 2017. Technical Report. <http://arxiv.org/abs/1705.07204>.
73. D. Tsipras, S. Santurkar, L. Engstrom, A. Turner, and A. Madry. Robustness may be at Odds with Accuracy, 2018. Technical Report. <http://arxiv.org/abs/1805.12152>.

74. C. Urban, M. Christakis, V. Wüstholtz, and F. Zhang. Perfectly Parallel Fairness Certification of Neural Networks. In *Proc. of the ACM on Programming Languages (OOPSLA)*, pages 1–30, 2020.
75. M. Usman, D. Gopinath, Y. Sun, Y. Noller, and C. Păsăreanu. NNrepair: Constraint-based Repair of Neural Network Classifiers, 2021. Technical Report. <http://arxiv.org/abs/2103.12535>.
76. S. Wang, K. Pei, J. Whitehouse, J. Yang, and S. Jana. Formal Security Analysis of Neural Networks using Symbolic Intervals, 2018. Technical Report. <http://arxiv.org/abs/1804.10829>.
77. Y. Wang, S. Jha, and K. Chaudhuri. Analyzing the Robustness of Nearest Neighbors to Adversarial Examples. In *Proc. 35th Int. Conf. on Machine Learning (ICML)*, pages 5120–5129, 2018.
78. E. Wong, L. Rice, and Z. Kolter. Fast is Better than Free: Revisiting Adversarial Training, 2020. Technical Report. <http://arxiv.org/abs/2001.03994>.
79. W. Xiang, H. Tran, and T. Johnson. Output Reachable Set Estimation and Verification for Multi-Layer Neural Networks. *IEEE Transactions on Neural Networks and Learning Systems (TNNLS)*, 2018.
80. H. Xiao, K. Rasul, and R. Vollgraf. Fashion-MNist: a Novel Image Dataset for Benchmarking Machine Learning Algorithms, 2017. Technical Report. <http://arxiv.org/abs/1708.07747>.
81. H. Xuan, R. Souvenir, and R. Pless. Deep Randomized Ensembles for Metric Learning. In *Proc. European Conf. on Computer Vision (ECCV)*, 2018.
82. X. Yang, T. Yamaguchi, H.-D. Tran, B. Hoxha, T. Johnson, and D. Prokhorov. Neural Network Repair with Reachability Analysis, 2021. Technical Report. <https://arxiv.org/abs/2108.04214>.
83. Y.-Y. Yang, C. Rashtchian, H. Zhang, R. Salakhutdinov, and K. Chaudhuri. A Closer Look at Accuracy vs. Robustness. In *Proc. Advances in Neural Information Processing Systems (NeurIPS)*, 2020.
84. X. Yu, B. Han, J. Yao, G. Niu, I. Tsang, and M. Sugiyama. How does Disagreement help Generalization against Label Corruption? In *Proc. 36th Int. Conf. on Machine Learning (ICML)*, pages 7164–7173, 2019.
85. H. Zhang, M. Shinn, A. Gupta, A. Gurfinkel, N. Le, and N. Narodytska. Verification of Recurrent Neural Networks for Cognitive Tasks via Reachability Analysis. In *Proc. 24th Conf. of European Conference on Artificial Intelligence (ECAI)*, 2020.
86. H. Zhang, Y. Yu, J. Jiao, E. Xing, L. El Ghaoui, and M. Jordan. Theoretically Principled Trade-off between Robustness and Accuracy. In *Proc. 36th Int. Conf. on Machine Learning (ICML)*, pages 7472–7482, 2019.
87. D. Zügner, A. Akbarnejad, and S. Günnemann. Adversarial Attacks on Neural Networks for Graph Data. In *Proc. 24th ACM SIGKDD Int. Conf. on Knowledge Discovery & Data Mining*, pages 2847–2856, 2018.



# Appendix

## A Verifying an Ensemble

Many modern DNN verification tools receive verification queries as  $\langle P, N, Q \rangle$  triples, where  $P$  is a precondition,  $N$  is the network to be verified, and  $Q$  is a postcondition. In order to verify a property of an ensemble  $\mathcal{E} = \{N_1, \dots, N_k\}$ , we must first transform the  $k$  networks into a single composite network  $N_{\mathcal{E}}$ , which can then be passed to the verifier. This construction is performed as follows:

- By definition, all ensemble members have the same input space, and so their input layers all have the same dimensions. The composite network  $N_{\mathcal{E}}$  will also have an input layer of the same dimension.
- Each network  $N_i$  is then placed within  $N_{\mathcal{E}}$ , with the composite network’s input layer serving as  $N_i$ ’s input layer. The  $N_i$  networks do not affect each other’s computation. In particular, the output layer of each  $N_i$  network becomes an internal, hidden layer of  $N_{\mathcal{E}}$ .
- The output layer of  $N_{\mathcal{E}}$  is constructed to reflect the ensemble’s aggregation mechanism. For simplicity, we focus here on the case where  $N_{\mathcal{E}}$  outputs the average of its constituent networks. In this case, if the networks’ output domain is of dimension  $t$ , network  $N_{\mathcal{E}}$ ’s output layer is a  $t$ -dimensional weighted sum layer; and its  $j$ ’th neuron,  $n_j$ , is computed as the weighted sum:

$$n_j = \sum_{i=1}^k \frac{1}{k} \cdot n_j^i,$$

where  $n_j^i$  is the  $j$ ’th output neuron of network  $N_i$ , currently encoded within  $N_{\mathcal{E}}$ .

An illustration of this process appears in Fig. 5. We note that similar variants of this construction have been applied in other contexts of DNN verification [39,53].

Once  $N_{\mathcal{E}}$  is constructed, it can be verified for different properties, e.g., adversarial robustness around a given input point  $x_0$ , using a standard encoding of that verification query.

## B Checking for Mutual Errors of Ensemble Members

Let  $N_1$  and  $N_2$  be two ensemble members, and suppose we wish to check whether these networks have a mutual error within a given  $\epsilon$ -ball  $B$  around point  $x_0$ , whose ground-truth label is  $l$ . We can achieve this as follows:

- We begin by constructing a composite network  $N_c$  that effectively evaluates  $N_1$  and  $N_2$ , side-by-side. This is similar to the process described in Section A, but with two differences. First, this time we only compose two networks, and so the blowup in size is not as significant. Second, we do not construct an

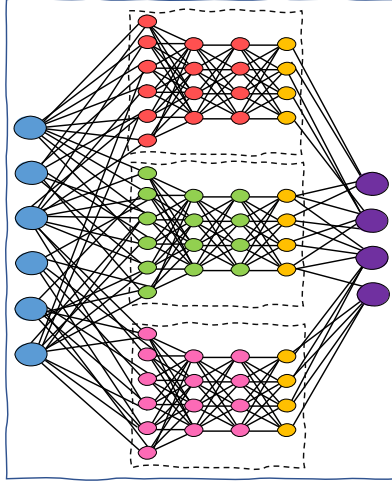


Fig. 5: An ensemble comprised of three different DNNs, each depicted in a different color. The input to the ensemble is passed, as is, to each of the individual DNN members, and the output of the ensemble is the average of the outputs of the individual members.

output layer that aggregates the outputs of  $N_1$  and  $N_2$ ; instead, the outputs of both  $N_1$  and  $N_2$  are concatenated into a single output layer of  $N_c$  (which is consequently twice as large as the output layers of  $N_1$  and  $N_2$ ).

- We use the precondition  $P$  to restrict the inputs of  $N_c$  to the  $\epsilon$ -ball  $B$ . Specifically, let  $x_0 = \langle x_0^1, \dots, x_0^n \rangle$ ; then:

$$P = \bigwedge_{i=0}^n |x^i - x_0^i| \leq \epsilon,$$

where  $x = \langle x^1, \dots, x^n \rangle$  is the input vector for  $N_c$ .

- We use the postcondition  $Q$  to ensure that both networks  $N_1$  and  $N_2$  misclassify input  $x$ ; that is, neither selects label  $l$  as its output. This is achieved by requiring that, among the outputs of  $N_1$ , the neuron that represents  $l$  is not assigned the maximal value; and likewise for  $N_2$ . More specifically, let  $y_1^1, \dots, y_r^1$  denote the outputs of  $N_1$ , and let  $y_1^2, \dots, y_r^2$  denote the outputs of  $N_2$ , so that the outputs of  $N_c$  are  $y_1^1, \dots, y_r^1, y_1^2, \dots, y_r^2$ . The postcondition  $Q$  in this case is

$$\bigvee_{i \neq l} (y_i^1 \geq y_l^1) \wedge \bigvee_{i \neq l} (y_i^2 \geq y_l^2)$$

Here,  $y_i^1$  and  $y_i^2$  represent the correct labels, and the postcondition requires that at least one other label be assigned a greater score, both in  $N_1$  and in  $N_2$ .

An illustration appears in Fig. 6. It is straightforward to show that the query  $\langle P, N_c, Q \rangle$  is SAT if  $N_1$  and  $N_2$  have a mutual error in  $B$ , and is UNSAT otherwise. This query can be dispatched using any number of existing DNN verification tools.

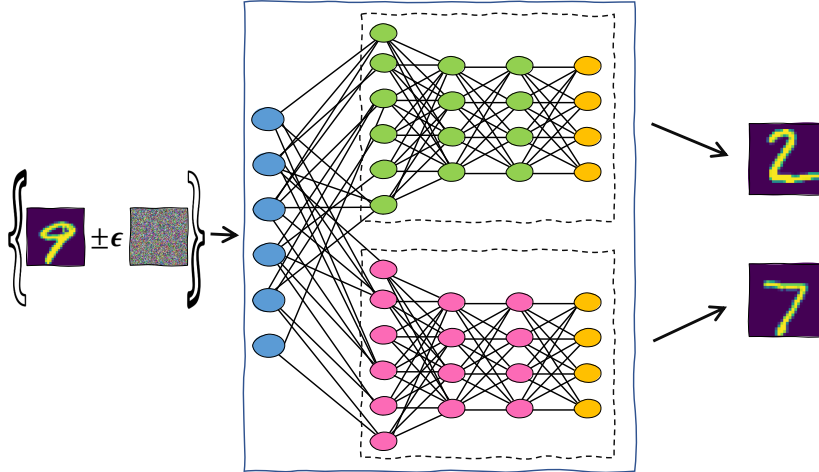


Fig. 6: Checking whether two MNIST digit recognition networks have a mutual error. The precondition restricts the inputs to an  $\epsilon$ -ball around a correctly classified digit “9”; the input is processed by the two networks independently; and the postcondition requires both networks to misclassify the input. In this case, one network outputs the incorrect label “2”, and the other network outputs the incorrect label “7”.

We note that in our experiments, we used the common practice of simplifying the query’s postcondition, by only considering the disjunct  $y_i \geq y_l$  for the label  $i$  that achieved the second-highest score on  $x_0$  (the “runner up”). This simplification is solely for the purpose of expediting the experiments; and the full postcondition could be encoded, as well.

## C Additional Evaluation Details

### C.1 MNIST

Our first set of experiments focused on the MNIST digit recognition dataset. Examples of inputs and perturbed inputs from this dataset appear in Figs. 7 and 8.

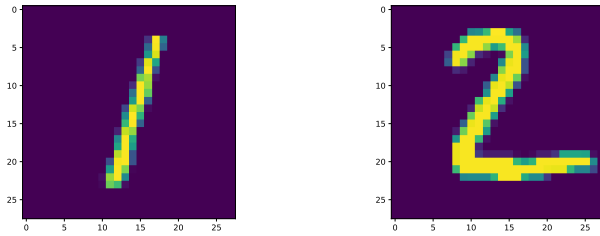


Fig. 7: Examples of two images from the MNIST dataset. The left image is labeled “1”, while the right image is labeled “2”. All images are  $28 \times 28$  grayscale images.

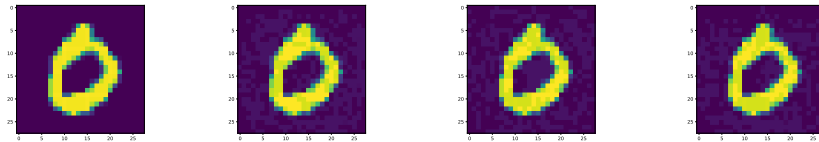


Fig. 8: Adversarial perturbations returned by the SAT verification queries in our experiments. From left to right are: a non-perturbed “0” image from the test set; and three  $\epsilon = 0.05$ -perturbations of the original image, causing misclassification by members  $N_1$  and  $N_2$  (second from the left), by members  $N_1$  and  $N_3$  (third from the left), and a misclassification by the whole ensemble  $\mathcal{E}_1 = \{N_1, N_2, N_3, N_4, N_5\}$  (on the right).

**Improving the Robust Accuracy of  $\mathcal{E}_1$ .** In order to improve the robust accuracy of  $\mathcal{E}_1$ , we computed the mutual error scores for each pair of ensemble members. This computation was performed by dispatching 1200 verification queries for every pair, using 6 different  $\epsilon$  values. The results appear in Table 2, grouped by network; e.g., the  $N_1$  column shows the aggregated results of all the pairwise queries where  $N_1$  appeared. Recall that a higher number of SAT results (or, equivalently, a lower number of UNSAT results) indicates that a network is more prone to simultaneous errors with its counterparts. These results were then used to compute the uniqueness score for each network, as presented in Table 3. Specifically, for the 200 inputs points, per pair, per  $\epsilon$  value, for each member  $N_t \in \mathcal{E}$ , we calculated the uniqueness score as:  $1 - (\#\text{SAT}) \cdot \frac{1}{200 \cdot |\mathcal{E} \setminus N_t|}$ .<sup>3</sup>

As the uniqueness scores show, network  $N_2$  obtains the lowest score (in bold) for each value of  $\epsilon$ , save for  $\epsilon = 0.01$ , where the margins are very small — presumably, because the small perturbation size prevents any of the networks from erring, almost at all. This clearly indicates that  $N_2$  is a prime candidate for replacement, although its original accuracy rate is actually highest among all networks comprising ensemble  $\mathcal{E}_1$  (see Table 3). Networks  $N_5$  and  $N_3$  are not far behind, often obtaining the second-lowest scores for the various epsilon values; whereas networks  $N_1$  and  $N_4$  are clearly the stronger of the lot. In our experiments we thus chose to replace  $N_2$  and  $N_5$ . After choosing the members to replace, we set out to search for the best replacement candidate from  $\mathcal{E}_2$ , relative to the remaining ensemble members. As an example, we supply the analysis at Table 4, indicating  $N_9$  is one of the two leading candidates to be added to  $\mathcal{E}_1 \setminus \{N_2\}$  and replace  $N_2$ , in order to improve the overall robust accuracy (see the left plot in Fig. 3).

Table 2: The results of the verification queries used to compute the mutual error scores of  $\mathcal{E}_1$ ’s constituent networks on the MNIST dataset. For each network  $N_i$ , the TIMEOUT values are:  $800 - (\#\text{SAT}) - (\#\text{UNSAT})$ .

$\epsilon$	$N_1$		$N_2$		$N_3$		$N_4$		$N_5$	
	# SAT	UNSAT	# SAT	UNSAT	# SAT	UNSAT	# SAT	UNSAT	# SAT	UNSAT
0.01	6	794	6	794	7	793	6	794	3	797
0.02	74	726	93	707	75	724	63	736	91	709
0.03	270	517	283	503	270	515	223	562	258	523
0.04	474	297	507	266	485	272	449	302	483	287
0.05	621	142	646	127	625	130	601	148	623	139
0.06	694	82	716	60	698	68	692	79	686	71

**Worsening the Robust Accuracy of  $\mathcal{E}_2$ .** Next, we conducted a similar analysis of the networks of  $\mathcal{E}_2$ ; the results appear in Tables 5 and 6. This time,

<sup>3</sup> In our experiments:  $|\mathcal{E} \setminus N_t| = 4$ , and the amount of all SAT queries for each member  $N_t$  is stated, per  $\epsilon$ , in Table 2.

Table 3: The uniqueness scores for the constituent networks of  $\mathcal{E}_1$  on the MNIST dataset. The minimal scores are in bold.

$\epsilon$	$N_1$	$N_2$	$N_3$	$N_4$	$N_5$
0.01	99.25	99.25	<b>99.13</b>	99.25	99.63
0.02	90.75	<b>88.38</b>	90.63	92.13	88.63
0.03	66.25	<b>64.63</b>	66.25	72.13	67.75
0.04	40.75	<b>36.63</b>	39.38	43.88	39.63
0.05	22.38	<b>19.25</b>	21.88	24.88	22.13
0.06	13.25	<b>10.5</b>	12.75	13.5	14.25

Table 4: The uniqueness scores for each replacing candidate from  $\mathcal{E}_2$ , relative to  $\mathcal{E}_1 \setminus \{N_2\}$ . The maximal scores are in bold.

$candidate \setminus \epsilon$	0.01	0.02	0.03	0.04	0.05	0.06
$N_6$	<b>99.88</b>	94.38	85.63	63.88	44.5	26.5
$N_7$	<b>99.88</b>	94.88	82.63	65.75	44.5	28.88
$N_8$	<b>99.88</b>	96.38	84.25	63.88	42	25
$N_9$	<b>99.88</b>	<b>97.88</b>	<b>89.13</b>	72	47.88	31.75
$N_{10}$	99.63	97.25	87.63	<b>74.63</b>	<b>55.25</b>	<b>39.25</b>

we set out to identify the strongest members of the ensemble. As the maximal entries (in bold) of Table 6 indicate, networks  $N_9$  and  $N_{10}$  obtain higher uniqueness scores than their counterparts. We selected  $N_4$  as the replacement for  $N_{10}$ , as our analysis (presented in Table 7) indicated that this member has a lower uniqueness score, relative to  $\mathcal{E}_2 \setminus \{N_{10}\}$ . We note that any of the  $\mathcal{E}_1$  members can worsen the robust accuracy, as our metrics indicate all members of  $\mathcal{E}_1$  achieve a lower uniqueness score than  $N_{10}$ , when inserted into  $\mathcal{E}_2 \setminus \{N_{10}\}$ . As expected, the total robust accuracy worsened when conducting the switch (see the right plot in Fig. 3).

Table 5: The results of the verification queries used to compute the mutual error scores of  $\mathcal{E}_2$ 's constituent networks on the MNIST dataset.

$\epsilon$	$N_6$		$N_7$		$N_8$		$N_9$		$N_{10}$			
	#	SAT	UNSAT	#	SAT	UNSAT	#	SAT	UNSAT	#	SAT	UNSAT
0.01	1	799	1	799	0	800	0	800	0	800		
0.02	21	779	26	774	20	780	9	791	18	782		
0.03	77	723	87	713	78	721	58	742	64	735		
0.04	199	601	202	598	201	599	162	638	166	634		
0.05	337	452	345	445	350	443	327	460	295	494		
0.06	484	301	489	293	503	288	464	315	430	345		

We observe that for all four novel ensembles we constructed ( $\mathcal{E}_1^{2 \rightarrow 9}$ ,  $\mathcal{E}_1^{5 \rightarrow 9}$ ,  $\mathcal{E}_2^{9 \rightarrow 4}$ ,  $\mathcal{E}_2^{10 \rightarrow 4}$ ), and presented in Fig. 3, the accuracy rates range between 97.7%

Table 6: The uniqueness scores for the constituent networks of  $\mathcal{E}_2$  on the MNIST dataset. The maximal scores are in bold.

$\epsilon$	$N_6$	$N_7$	$N_8$	$N_9$	$N_{10}$
0.01	99.88	99.88	<b>100</b>	<b>100</b>	<b>100</b>
0.02	97.38	96.75	97.5	<b>98.88</b>	97.75
0.03	90.38	89.13	90.25	<b>92.75</b>	92
0.04	75.13	74.75	74.88	<b>79.75</b>	79.25
0.05	57.88	56.88	56.25	59.13	<b>63.13</b>
0.06	39.5	38.88	37.13	42	<b>46.25</b>

Table 7: The uniqueness scores for each replacing candidate from  $\mathcal{E}_1$ , relative to  $\mathcal{E}_2 \setminus \{N_{10}\}$ . The minimal scores are in bold.

$candidate \setminus \epsilon$	0.01	0.02	0.03	0.04	0.05	0.06
$N_1$	100	96.38	85.25	66.25	45	27.38
$N_2$	<b>99.75</b>	95.25	84.75	<b>63.5</b>	<b>41.25</b>	<b>26.13</b>
$N_3$	<b>99.75</b>	96.38	84.75	65.13	43.13	26.75
$N_4$	99.88	95.75	87.75	69	46.75	29.5
$N_5$	99.88	<b>95</b>	<b>83.88</b>	65.13	44	28.5

and 98.7% — i.e., were higher than the accuracy rates of each of the individual DNNs comprising them. We also observe that there is a slight negative correlation between an ensemble’s robust accuracy and its accuracy: by improving the robust accuracy of an ensemble, we risk slightly decreasing its accuracy, and vice versa. This finding is in accordance with previous research [73].

## C.2 Fashion-MNIST

As mentioned in Section 4, we repeated the process on additional networks, trained on the Fashion-MNIST dataset (examples of inputs and perturbed inputs from this dataset appear in Figs. 9 and 10). In this experiment, we noticed a low variance among the relative uniqueness scores of the members comprising  $\mathcal{E}_3$ , compared to a larger variance among the relative uniqueness scores of the members comprising  $\mathcal{E}_4$ . This led us to focus on  $\mathcal{E}_4$ , in order to check whether our method allows improving (or worsening) the ensemble’s robust accuracy. The high variance among the uniqueness scores of  $\mathcal{E}_4$ ’s members can be seen in Table 8.

The mutual error scores of  $\mathcal{E}_3$ ’s members appear in Table 9, and these give rise to the uniqueness scores displayed in Table 10. For  $\mathcal{E}_4$ , the mutual error scores appear in Table 11, and the uniqueness scores appear in Table 12. As can be seen, member  $N_{18}$  is the most unique member of  $\mathcal{E}_4$ , and replacing it with  $N_{13}$ , a member from  $\mathcal{E}_3$  with a low uniqueness score (see Table 13), worsens the robust accuracy. In the opposite direction, for almost all  $\epsilon$ -sized perturbations,  $N_{20}$  is the least unique member, and replacing it with  $N_{15}$ , a member from  $\mathcal{E}_3$  with a higher uniqueness score (see Table 14), increases the robust accuracy. As

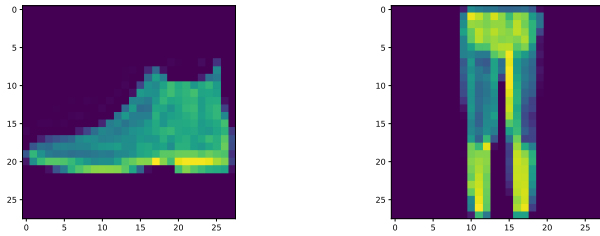


Fig.9: Examples of two images from the Fashion-MNIST dataset of clothing items. The left image is labeled “Sneaker”, while the right image is labeled “Trousers”. All images are  $28 \times 28$  grayscale images.

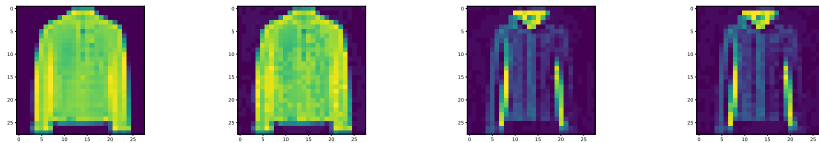


Fig.10: An image from the Fashion-MNIST dataset labeled as a “coat” (first on the left), and an  $\epsilon = 0.04$ -perturbation of that image misclassified by  $\mathcal{E}_3$  (second on the left). The two images on the right are two adversarial examples of another “coat”-labeled image, which cause a joint error for the pairs  $(N_{13}, N_{14})$  and  $(N_{14}, N_{15})$ .



Table 8: Accuracy and uniqueness scores for the Fashion-MNIST networks. Uniqueness scores are measured with respect to the ensemble (either  $\mathcal{E}_3$  or  $\mathcal{E}_4$ ).

	$\mathcal{E}_3$					$\mathcal{E}_4$				
	$N_{11}$	$N_{12}$	$N_{13}$	$N_{14}$	$N_{15}$	$N_{16}$	$N_{17}$	$N_{18}$	$N_{19}$	$N_{20}$
Accuracy	87.14%	87.13%	87.53%	87.34%	87.3%	87.05%	87.32%	87.35%	87.34%	87.11%
US	70.63%	71.5%	<b>69.75%</b>	70.88%	<b>73.25%</b>	67.38%	72.38%	<b>80.13%</b>	71.38%	<b>66.75%</b>

Table 9: The results of the verification queries used to compute the mutual error scores of  $\mathcal{E}_3$ 's constituent networks on the Fashion-MNIST dataset.

$\epsilon$	$N_{11}$		$N_{12}$		$N_{13}$		$N_{14}$		$N_{15}$	
	# SAT	UNSAT	# SAT	UNSAT	# SAT	UNSAT	# SAT	UNSAT	# SAT	UNSAT
0.01	43	757	40	760	48	752	43	757	28	772
0.02	235	565	228	572	242	558	233	567	214	586
0.03	493	307	437	363	484	316	469	331	435	365
0.04	651	148	611	188	655	145	629	171	610	190
0.05	759	38	720	75	758	40	745	53	736	58
0.06	795	3	789	8	793	4	785	8	788	7

in the MNIST experiments, the uniqueness scores of the replacing members are always compared to the remaining members. The robust accuracy changes are presented in Fig. 4.

Our results for Fashion-MNISNT suggest that an ensemble that attains high robust accuracy on different agreement points with *the same* label (“coat”, in our experiments) also achieves high accuracy on points from the test data for which this is the correct label (even if these are not agreement points). We note, however, that our results also indicate that, unlike in the MNIST case, robust accuracy with respect to data points with one label does not imply robust accuracy with respect to points with *a different* label. This is not surprising; classification for the Fashion-MNISNT dataset is more challenging, and so there is no reason to expect that two members of an ensemble that rarely err together on the region of the input that corresponds to a certain label, also seldom err simultaneously on other regions. Our results suggest that to attain high robust accuracy with respect to the underlying distribution, the choice of ensemble should be done on a validation set that consists of agreement points whose labels are distributed similarly to the empirically observed distribution in the training data (which is expected to approximate the underlying distribution).

Table 10: The uniqueness scores for the constituent networks of  $\mathcal{E}_3$  on the Fashion-MNIST dataset.

$\epsilon$	$N_{11}$	$N_{12}$	$N_{13}$	$N_{14}$	$N_{15}$
0.01	94.63	95	94	94.63	96.5
0.02	70.63	71.5	69.75	70.88	73.25
0.03	38.38	45.38	39.5	41.38	45.63
0.04	18.63	23.63	18.13	21.38	23.75
0.05	5.13	10	5.25	6.88	8
0.06	0.63	1.38	0.88	1.88	1.5

Table 11: The results of the verification queries used to compute the mutual error scores of  $\mathcal{E}_4$ 's constituent networks on the Fashion-MNIST dataset.

$\epsilon$	$N_{16}$			$N_{17}$			$N_{18}$			$N_{19}$			$N_{20}$		
	#	SAT	UNSAT	#	SAT	UNSAT	#	SAT	UNSAT	#	SAT	UNSAT	#	SAT	UNSAT
0.01	75	725	48	752	30	770	45	755	72	728					
0.02	261	539	221	579	159	641	229	571	266	534					
0.03	529	271	494	306	441	359	491	309	529	271					
0.04	692	108	672	128	633	167	664	136	685	115					
0.05	774	26	753	47	739	59	756	43	770	29					
0.06	793	5	787	10	780	19	790	9	792	7					

Table 12: The uniqueness scores for the constituent networks of  $\mathcal{E}_4$  on the Fashion-MNIST dataset.

$\epsilon$	$N_{16}$	$N_{17}$	$N_{18}$	$N_{19}$	$N_{20}$
0.01	90.63	94	96.25	94.38	91
0.02	67.38	72.38	80.13	71.38	66.75
0.03	33.88	38.25	44.88	38.63	33.88
0.04	13.5	16	20.88	17	14.38
0.05	3.25	5.88	7.63	5.5	3.75
0.06	0.88	1.63	2.5	1.25	1

Table 13: The uniqueness scores for each replacing candidate from  $\mathcal{E}_3$ , relative to  $\mathcal{E}_4 \setminus \{N_{18}\}$ . The minimal scores are in bold.

$candidate \setminus \epsilon$	0.01	0.02	0.03	0.04	0.05	0.06
$N_{11}$	<b>90.75</b>	66.75	<b>31.5</b>	<b>14.38</b>	<b>3.38</b>	<b>0.5</b>
$N_{12}$	94.25	69.25	44.63	20.5	9.25	2.13
$N_{13}$	91.25	<b>66.5</b>	34.88	15.13	3.75	0.63
$N_{14}$	92.75	66.88	36.88	18.13	5.75	1.38
$N_{15}$	96.25	72.88	43.88	21.5	6.75	0.88

Table 14: The uniqueness scores for each replacing candidate from  $\mathcal{E}_3$ , relative to  $\mathcal{E}_4 \setminus \{N_{20}\}$ . The maximal scores are in bold.

<i>candidate</i> \ $\epsilon$	0.01	0.02	0.03	0.04	0.05	0.06
$N_{11}$	92.63	71.5	35.88	16.38	4.38	1.13
$N_{12}$	95.25	73.63	<b>47.5</b>	21.63	<b>10</b>	<b>3</b>
$N_{13}$	93	70.63	38.75	16.5	4.63	1.13
$N_{14}$	94.5	71.38	41	19.75	6.38	1.63
$N_{15}$	<b>96.75</b>	<b>76.25</b>	46.5	<b>23.25</b>	7.88	1.63